HHS Public Access

Author manuscript

Chemistry. Author manuscript; available in PMC 2017 June 06.

Published in final edited form as:

Chemistry. 2016 June 06; 22(24): 8158–8166. doi:10.1002/chem.201600674.

Discovery, Total Synthesis and Key Structural Elements for the Immunosuppressive Activity of Cocosolide, a Symmetrical Glycosylated Macrolide Dimer from Marine Cyanobacteria

Dr. Sarath P. Gunasekera[a],+, **Yang Li**[b],+, **Dr. Ranjala Ratnayake**[c],+, **Danmeng Luo**[c], **Dr. Jeannette Lo**[d], **Dr. Joseph H. Reibenspies**[e], **Dr. Zhengshuang Xu**[b], **Prof. Dr. Michael J. Clare-Salzler**[d], **Prof. Dr. Tao Ye***,[b], **Dr. Valerie J. Paul***,[a], and **Prof. Dr. Hendrik Luesch***,[c]

[a]Smithsonian Marine Station, 701 Seaway Drive, Fort Pierce, Florida 34949, United States

[b]Laboratory of Chemical Genomics, School of Chemical Biology and Biotechnology, Shenzhen Graduate School of Peking University, Shenzhen 518055, P.R. China

[c]Department of Medicinal Chemistry & Center for Natural Products, Drug Discovery and Development (CNPD3), University of Florida, Gainesville, Florida 32610, United States

[d]Department of Pathology, Immunology and Laboratory Medicine, University of Florida, Gainesville, Florida 32610, United States

[e]Department of Chemistry, Texas A & M University, College Station, Texas 77843, United States

Abstract

A new dimeric macrolide xylopyranoside, cocosolide (**1**), was isolated from the marine cyanobacterium preliminarily identified as *Symploca* sp. from Guam. The structure was determined by a combination of NMR, HRMS, X-ray diffraction studies and Mosher's analysis of the base hydrolysis product. Its carbon skeleton closely resembles that of clavosolides A–D isolated from the sponge *Myriastra clavosa*, for which no bioactivity is known. We performed the first total synthesis of cocosolide (**1**) along with its [α,α]-anomer (**26**) and macrocyclic core (**28**), thus leading to the confirmation of the structure of natural **1**. The convergent synthesis featured Wadsworth–Emmons cyclopropanation, Sakurai annulation, Yamaguchi macrocyclization/dimerization reaction, α-selective glycosidation and β-selective glycosidation. Compounds **1** and **26** potently inhibited IL-2 production in both T-cell receptor dependent and independent manners. Full activity requires the presence of the sugar moiety as well as the intact dimeric structure. Cocosolide (**1**) also suppressed the proliferation of anti-CD3-stimulated T-cells in a dose-dependent manner.

Diving into symmetry

+These authors contributed equally to this work.

Supporting information for this article is available on the *WWW* under ……

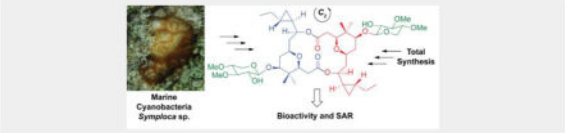

A new dimeric macrolide xylopyranoside, cocosolide, was isolated from marine cyanobacteria. Its structure was elucidated by a combination of spectroscopic methods and further confirmed by total synthesis. Along with its [α,α]-anomer and macrocyclic core, cocosolide was evaluated in various bioassays, which unveiled its role in immunosuppression. SAR study indicated the presence of the sugar moiety and the intact dimeric structure was required to achieve full activity.

Keywords

marine natural products; glycosides; macrolides; structure determination; total synthesis

Introduction

The chemical diversity of secondary metabolites reported to date has shown that marine cyanobacteria are an excellent resource for the discovery of new compounds.[1] Furthermore, marine cyanobacteria have been shown to be a source for secondary metabolites with interesting bioactivities and mechanisms of action.[2,3] In our continuing search for new metabolites from marine cyanobacteria, we have isolated a macrolide xylopyranoside trivially named cocosolide (**1**) from the lipophilic extracts of the soft, golden cyanobacterium preliminarily identified as *Symploca* sp. collected from Cocos Lagoon and Tanguisson reef flat, Guam. Cocosolide (**1**) is a symmetrical dimer, which structurally resembles the sponge metabolites clavosolides A-D isolated from a Philippine collection of the sponge *Myriastra clavosa*[4,5] and cyanolide A obtained from a Papua New Guinea collection of *Lyngbya bouillonii* (Figure 1).[6] Symmetrical dimeric secondary metabolites are rare in marine cyanobacteria. Two related symmetrical dimeric compounds tanikolide dimer[7] and malyngolide dimer[8] were reported from *Lyngbya majuscula* collected from Malagasy and Panama, respectively. To our knowledge, this is the second report of a dimeric macrolide glycoside isolated from cyanobacteria. An additional unusual structural feature is the presence of cyclopropyl groups, previously encountered in only a few cyanobacterial metabolites.[9] We report herein the details of isolation, structure elucidation, X-ray diffraction data of cocosolide (**1**), total synthesis and the biological activity studies of cocosolide (**1**), its anomer **26**, monomeric analogues **2** and **3**, and aglycon **28** (macrocyclic core).

Results and Discussion

Isolation and structure determination

The initial sample of the marine cyanobacterium *Symploca* sp., which appears as soft golden puffballs, was collected from a patch reef in Cocos Lagoon, Guam. The freeze-dried material was successively extracted with a mixture of CH_2Cl_2-MeOH (1:1) and aqueous MeOH (1:1). The combined extract was subsequently partitioned between EtOAc and H_2O.

The EtOAc-soluble portion was repeatedly fractionated by SiO_2 chromatography followed by reversed-phase C18 HPLC to give a new compound, cocosolide (**1**, 8.0 mg, 0.08 % extract wt). Crystallization of cocosolide (**1**) in 10% EtOAc-hexanes furnished colorless crystals, and **1** indicated negative specific rotation similar to the previously described clavosolides.[4,5] The molecular formula of (−)-cocosolide (**1**) $C_{46}H_{76}O_{16}$ was established from a high resolution ESIMS measurement of the $[M + Na]^+$ peak at *m/z* 907.5009. Since the ^{13}C spectrum (Table 1) showed only 23 signals, it was evident that **1** was a symmetrical dimer. The IR spectrum indicated the presence of alcohol, ester and ether functionalities by IR bands at 3462, 1741 and 1073 cm^{-1}, respectively. Following the interpretation of DQF COSY and edited HSQC experiments, the ^1H and ^{13}C NMR signals were assignable to three partial structures C-2 to C-3, C-5 to C-14 and C-17 to C-21. The presence of a high-field methylene group H_2-14 (δ_H 0.37, 0.23) that was coupled to two mutually coupled high-field methines H-10 (δ_H 0.68) and H-11 (δ_H 0.71) indicated the existence of a disubstituted cyclopropyl group in the C-5 to C-14 partial structure.

In addition, the ^1H NMR spectrum indicated two singlets corresponding to two *O*Me groups (δ, 3.49, 3.38) and another two singlets corresponding to two methyl groups (δ, 0.87, 0.79). The large geminal coupling constant (J = 17.2 Hz) for the H_2-2 methylene protons indicated that this methylene group is adjacent to the ester carbonyl.[5] HMBC correlations (Table 1) from H_2-2 (δ_H 2.38, 2.07) and H-3 (δ_H 3.40) to C-1 ester carbonyl (δ_C 171.7) and from H_2-2a to C-4 quaternary carbon (δ_C 39.2) connected these two quaternary carbons to partial structure C-2 to C-3. The two methyl groups showed HMBC correlations to each other indicating the geminal arrangement of these methyl groups. Further HMBC correlations of these two methyls to C-3, C-4 and C-5 and HMBC correlation between H_2-6 and C-4 linked C-4 to C-5 and thus established the C-1 to C-14 carbon skeleton. The partial structure C-17 to C-21 was identified as a pyranose sugar through HMBC correlation of the oxymethylene H_2-21(δ_H 3.90, 3.09) to the C-17 (δ_C 106.4) anomeric carbon. The large diaxial coupling constant values (Table 1) observed for all oxymethines including the anomeric proton H-17 (J = 7.6 Hz) established a β-xylopyranose residue. HMBC correlations connected the two methoxy groups H_3-22 (δ 3.49) and H_3-23 (δ 3.38) to C-19 (δ_C 85.4) and C-20 (δ_C 80.0), respectively. The free OH group at δ_H 3.33 showed a COSY correlation to H-18 and HMBC correlation to C-17 and C-19, and therefore the position of the OH group was assigned to C-18. The oxymethine H-5 (δ_H 3.34) showed HMBC correlation to the anomeric carbon C-17 of the sugar moiety indicating the position of connectivity. Absence of other hydroxyl groups in the molecule and the HMBC correlation seen from H-3 to C-7 showed that C-3 through C-7 formed the tetrahydropyran ring. HMBC correlation between oxymethine H-9 and carbonyl carbon C-1 indicated the ester link at this position. These data established the symmetric 16-membered macrocyclic planar structure for cocosolide (**1**).

The relative stereostructure of cocosolide (**1**) was determined by single crystal X-ray diffraction. Cocosolide (**1**) is structurally related to the sponge metabolites clavosolides A-D. This unique structure of the clavosolides attracted many synthetic chemists. Willis and coworkers[10] in 2005 and Chakraborty and Reddy[11] in 2006 reported the total synthesis of (−)-clavosolide A. Both groups observed discrepancies in the ^1H NMR spectrum in the cyclopropyl region between the natural product and their synthetic compound and

reassigned the cyclopropyl carbinyl stereogenicity of the natural product. During the same period Smith and Simov[12] synthesized the revised structure of (−)-clavosolide A. The ^{1}H and ^{13}C NMR data of their synthetic (−)-clavosolide A proved to be in perfect agreement with the corresponding data reported for the natural (−)-clavosolide A.[5] The relative stereochemistry of the synthetic (−)-clavosolide A was confirmed by X-ray crystallography. The absolute stereochemistry of (−)-clavosolide A was assigned based on the absolute configuration of D-(+)-xylose, employed in the synthesis. The X-ray crystallography data of (−)-cocosolide (**1**) are in full agreement with the corresponding data reported for synthetic (−)-clavosolide A[12] for all stereogenic centers (Figure 2, Supporting Information Table S1). Therefore, we established the relative configuration for all stereogenic centers of the structure of (−)-cocosolide (**1**) based on the absolute configuration of synthetic (−)-clavosolide A.

Base hydrolysis of cocosolide (**1**) furnished the monomer **2** (Figure 3). Methylation of **2** with CH_2N_2 gave the methyl ester **3** (Figure 3). The structures of compounds **2** and **3** were determined by NMR studies and confirmed by HRMS studies. These two monomeric compounds **2** and **3** were prepared specifically for structure activity relationship studies, and subsequently the compound **3** was used to prepare the Mosher esters to establish the absolute stereochemistry of (−)-cocosolide (**1**). The two secondary hydroxy groups at C-9 and C-18 in compound **3** gave MTPA diesters. The MTPA ester of the sugar moiety (C-18) did not interfere with the stereochemical analysis given, and the $\Delta\delta$ values shown in Figure 3 indicated the absolute configuration at C-9 was *S*. Applying this stereochemical information in the X-ray crystallography data established the absolute stereochemistry for all stereogenic centers in (−)-cocosolide (**1**).

Following its consistent isolation from subsequent Cocos Lagoon collections, we also encountered the same cocosolide- producing cyanobacterium at other collection sites, including the reef flat at Tanguisson, Piti, Fingers Reef, and north of Pago Bay. The cyanobacterium occurs in many shallow reef habitats around the island of Guam.

Total synthesis of cocosolide, its [α,α]anomer and macrocyclic core

Retrosynthetic analysis—Literature precedent for the synthesis of (−)-clavosolide A and (−)-cyanolide A indicated that the glycosylation of the symmetrical parent diol of a bis-macrolactone precursor led to a statistical mixture of [α,α]-, [β,β]-, and [α,β]-anomers, which reduced the overall yield of the total synthesis.[13–16] Thus, in designing the synthetic strategy to cocosolide we aimed to close the macrocycle via the dimerization of the permethylated-D-xylose-containing monomer **21**, which could be obtained from glycosylation of alcohol **19**. The Sakurai reaction of allylsilane **9** and aldehyde **12** was anticipated to stereoselectively provide a 3,3-disubstituted 2,6-*cis*-tetrahydropyran precursor **17**, which was readily converted into **19** by oxidative cleavage of the double bond and subsequent reduction of the resulting ketone. The required allylsilane **9** could be derived from the known β-hydroxy ester **4**.[17] The key intermediate **12** would be established through an asymmetric allylation of an appropriate aldehyde derived from the cyclopropane-containing acid **11** (Figure 4).

Synthesis of allylsilane 9—The synthesis of fragment **9** started with the protection of the known chiral ester **4**[17] as its triethylsilyl (TES) ether, followed by treatment of the methyl ester with trimethylsilylmethyllithium to give methyl ketone **6** in 83% yield over two steps[18–23] (Scheme 1). Treatment of ketone **6** with KHMDS and *N*-phenyltrifluoromethanesulfonimide afforded enol triflate **7** in 91% yield. Kumada coupling of enol triflate **7** with (trimethylsilyl)methyl Grignard reagent and selective desilylation of TES ether in the presence of a catalytic amount of CSA gave allylsilane **9** in 61% overall yield.

Synthesis of aldehyde 12—With the key intermediate **9** in hand, we next turned our attention to the synthesis of aldehyde **12**, which contains a *trans*-disubstituted-cyclopropane moiety (Scheme 2). Thus, commercially available (*S*)-2-ethyloxirane **10** was subjected to optimized Wadsworth–Emmons cyclopropanation followed by an in situ saponification to furnish acid **11** in 82% yield.[24–28] This acid was then converted into homoallylic alcohol **11a** via a three-step sequence involving a $LiAlH_4$ reduction to furnish the corresponding alcohol, a TEMPO promoted oxidation to give rise to an aldehyde and Brown allylation to set the third stereocenter. Protection of the homoallylic alcohol of **11a** as its benzyl ether, followed by oxidative cleavage of the terminal olefin with OsO_4 and $NaIO_4$ to produce the required aldehyde **12** in 26% overall yield from **11**.

Synthesis of thioglycoside 16—Thioglycosyl donor **16** was accessed from the known ortho ester **14** as shown in Scheme 3. Treatment of ortho ester **14** with thiophenol in the presence of $BF_3{\cdot}OEt_2$ afforded thioglycoside **15** in 36% yield.[29,30] Hydrolysis of the acetate group in **15** and reprotection of the resulting secondary alcohol with *tert*-butyldimethylsilyl triflate afforded the desired thioglycosyl donor **16** in 86% yield.

Assembly of subunits and completion of the synthesis of cocosolide (1)—With allylsilane **9**, aldehyde **12** and thioglycoside **16** in hand, we were poised to complete the synthesis of cocosolide (**1**) (Scheme 4). The TMSOTf-promoted Sakurai annulation of allylsilane **9** with aldehyde **12**, was found to occur rapidly at −78 °C to provide the 2,6-*cis*-tetrahydropyran (**17**) containing an *exo*-methylene in the 4-position. It is also worth noting that, most recently Millán et.al reported a concise methodology to construct the tetrahydropyran motif by using a three-component allylboration-Prins reaction sequence, which may provide us an opportunity to further optimize our synthetic scheme.[31] Dihydroxylation of **17** using the Upjohn method[32,33] and subsequent periodate cleavage afforded **18** in 85% yield. Reduction of the ketone with sodium borohydride gave rise to the secondary alcohol **19** in 92% yield as a single diastereomer.[12] Treatment of thioglycoside **16** with one equivalent of NBS at −25 °C in dry acetonitrile, followed by addition of aglycone (**19**), the glycosidation proceeded with 5:3 β-selectivity afforded the desired β-anomer **20** in 60% isolated yield.[34–37] Subsequent removal of the bis-benzyl ethers under hydrogenative conditions gave rise to diol **21**. The primary alcohol in **21** was selectively converted into the corresponding acid with a one-step TEMPO-catalyzed oxidation protocol.[38] Macrodiolide formation under Yamaguchi's conditions[39] provided macrocycle **22** in 43 % yield over two steps. Deprotection of **22** with TBAF in THF then furnished cocosolide (**23**), which was identical to the natural product in all respects.

Synthesis of [α,α]-anomer of cocosolide (26)—With both **19** and **16** in hand, we prepared the [α,α]-anomer of cocosolide using the same strategy (Scheme 5),wherein, a highly α-selective glycosidation of aglycone **19** with thioglycoside **16** was achieved under the promotion of NIS, TfOH in CH_2Cl_2 to furnish the desired α-anomer **23** in 71% isolated yield.[40] Intermediate **23** was then elaborated to the [α,α]-anomer of cocosolide (**26**) in 19% yield by an identical strategy as described for **1**, including removal of bis-benzyl ether, TEMPO-catalyzed oxidation, macrodiolide formation and desilylation. (Scheme 5).

Synthesis of macrocyclic core of cocosolide (28)—The macrocyclic core of cocosolide (**28**) was prepared from **19** by a similar strategy as described for **1**. Thus, protection of the secondary alcohol as its *tert*-butyldimethylsilyl (TBS) ether, followed by removal of the bis-benzyl ethers under hydrogenative conditions gave rise to the corresponding diol, which was then selectively converted into the corresponding acid with a one-step TEMPO-catalyzed oxidation protocol. Direct macrocyclization using Yamaguchi's conditions afforded the C_2 symmetric diolide **27** in 19% yield over four steps. Deprotection of **27** with TBAF in THF then furnished **28** in 71% yield.

Biological studies—To study the effect of cocosolide (**1**) on biological function, we treated an array of cell types (HCT116 colorectal cancer cells, RAW macrophage cells, Jurkat T-cell lymphoma cells; IC_{50} > 50 μM) with cocosolide (**1**) and found no modulation of cell viability. Structural considerations, including the dimeric nature coupled with the glycosylation feature, hinted at the possibility of dimeric surface targets for geometric and recognition consideration, respectively. We tested the effects in immortalized T-cells (Jurkat) as a model to evaluate immunomodulatory activity.[41] IL-2 production was induced via dual stimulation with phorbol 12-myristate 13-acetate (PMA, 80 nM) and phytohemagglutinin (PHA, 10 μg/mL), conditions for a T-cell receptor (TCR) dependent activation; or TCR-independent stimulants PMA (80 nM) and ionomycin (1 μM).[42] Cocosolide (**1**) and its [α,α]-anomer (**26)** equally and potently reduced IL-2 production without significantly affecting cell viability (Figures 5A and B). The susceptibility of the TCR-independent system was stronger, although both stimulations are abrogated in a dose-dependent manner. The macrocyclic core **28** and monomer ester **3** showed minimal effects in these assays compared with **1** and **26** (Figures 5C and D), indicating that the sugar and dimeric structure are important to the target recognition and engagement process.

To examine how cocosolide (**1**) may affect activated T cells, we stimulated spleen cells with CD3 and cultured the cells under increasing concentrations of cocosolide (**1**) for 72 h. As shown in Figure 5E, cocosolide (**1**) inhibited anti-CD3-mediated T-cell proliferation in a dose-dependent manner. Cell viability was not affected compared with DMSO-treated controls, suggesting that the observed suppression of T cell expansion by **1** is not attributed to cell death.

We also investigated possible modulation of Toll-like receptor 4 mediated pathways. Specifically, RAW264.7 macrophage cells were stimulated with lipopolysaccharides (LPS), and pretreatment with cocosolide (**1**) did not dampen the induction of NO production and also did not reduce the viability (up to 100 μM). Similarly, **1** did not exert antibacterial

activity in our assays (*Bacillus cereus*, *Pseudomonas aeruginosa*, *Mycobacterium tuberculosis*). Taken together, cocosolide's effects appear to be fairly cell- and pathway-type specific.

The non-cytotoxic effects are consistent with data reported for the structurally related clavosolides, for which a bioactivity remained to be established.[4,5] Clavosolides A and B were first reported from the sponge *Myriastra clavosa* but suggested to be of cyanobacterial origin because the structure did not relate to any known sponge metabolites and the presence of a high concentration of cyanobacterial cells was found in the sponge sample.[5] These dimeric metabolites along with two other analogues, clavosolides C and D were concurrently reported by a second group also from a cytotoxic extract of *M. clavosa*, displaying differential cytotoxicity in the NCI-60 cell panel.[4] Evaluation of the purified compounds revealed that these are non-cytotoxic. The structurally related macrolide cyanolide A was reported from the cyanobacterium *L. bouillonii* with potent molluscicidal activity against *Biomphalaria glabrata*, but non-cytotoxic effects against H-460 human lung adenocarcinoma and mouse neuroblastoma cells.[6]

Conclusions

This discovery of cocosolide (**1**) and the recent report of cyanolide A in a marine cyanobacterium verify the possible cyanobacterial origin for the related clavosolides. Rigorous biological studies necessitated an efficient total synthesis with a high degree of selectivity for the key steps and access to key analogues to probe structural requirements. We have achieved first total synthesis of cocosolide (**1**) along with its [α,α]-anomer (**26**) and macrocyclic core (**28**), thus leading to the confirmation of the structure of natural cocosolide. The convergent synthesis features Wadsworth–Emmons cyclopropanation, Sakurai annulation, Yamaguchi macrocyclization/dimerization reaction, α-selective glycosidation and β-selective glycosidation. The synthesis provided further quantities of the natural product and structural derivatives for biological studies. Initial biological studies suggested an immunosuppressive activity based on inhibition of IL-2 production and T-cell proliferation. Preliminary structure–activity relationship studies indicated the importance of the dimeric macrolide core and the glycosylation. Studies towards the mechanism of action and investigation of other biological effects are ongoing.

Experimental Section

Cocosolide (1)—Colorless crystals; mp 233–234 °C; $[\alpha]^{25}_{D}$ −65.3 (*c* 0.41, CH_2Cl_2); UV (MeOH) λ_{max} (log ε) 210 (3.39) nm; IR (film) ν_{max} 3462, 2957, 1741, 1464, 1252, 1165, 1096, 1073, 953 $cm^{-1;}$ ^1H NMR, ^{13}C NMR, DQF COSY, HMBC and NOESY data, see Table 1; HRESI/APCIMS *m*/*z* 907.5009 $[M + Na]^+$ (calcd for $C_{46}H_{76}O_{16}Na$, 907.5026). Comparison of ^1H and ^{13}C NMR spectra of cocosolide (**1**) from Cocos Lagoon and Tanguisson reef flat are shown in Supporting Information, Figures S1 and S2.

Biological reagents and general experimental procedures—Phorbol myristate acetate (PMA) was purchased from Promega (Cat# V1171; Madison, WI). Phytohemagglutinin (PHA) was from Sigma-Aldrich (Cat# L8902; St. Louis, MO) and

ionomycin, calcium salt was purchased from EMD Chemicals, Inc (cat# 407952; Gibbstown, NJ). Human colon adenocarcinoma HCT116 cells and the human leukemic T-cell line Jurkat (Clone E6-1) were obtained from the American Type Culture Collection (Manassas, VA) and cultured either Dulbecco's modified Eagle's medium (Invitrogen, Carlsbad, CA) for HCT116 cells and RPMI 1640 medium (Cellgro, Herndon, VA) for Jurkat cells, supplemented with 10% fetal bovine serum (HyClone Laboratories, Logan, UT). Cells were maintained at 37 °C humidified air in 5% CO_2.

Cell viability assays—HCT116, RAW 264.7 and Jurkat cells were seeded in 96-well plates and 24 h later treated with up to 50 μM cocosolide (**1**) for 24 h (RAW 264.7) or 48 h (HCT116, Jurkat). Cell viability was measured using MTT reagent according to the manufacturer's instructions (Promega, Madison, WI, USA).

Measurement of IL-2 production (Jurkat cells)—Jurkat cells (1×10^5 cells per well; 150 μL each well) were seeded in 96-well clear bottom plates and allowed to settle for one hour. Cells were then co-treated with compounds **1**, **3**, **26** and **28** (50 μM to 100 nM in EtOH) and TCR-dependent stimulants (80 nM PMA in DMSO and 10 μg/ml PHA in H_2O) or TCR-independent stimulants (80 nM PMA in DMSO and 1 μM ionomycin in DMSO) along with EtOH/DMSO solvent controls. Cells were also treated with compounds alone to measure cell viability due to PMA/PHA and PMA/ionomycin toxicities. DMSO concentrations were maintained at 0.21% to minimize toxicity for Jurkat cells. After 24 h incubation, 50 μL of culture supernatant were removed from each well into a separate plate and used for measuring IL-2 production using an alphaLISA kit (PerkinElmer, Waltham, MA). Briefly, acceptor bead and anti-IL-2 antibody were incubated with 5 μL of supernatant for 60 min and donor beads added and incubated for further 30 min following which, IL-2 was quantified using Envision-Reader (PerkinElmer). The cells were used to measure viability after 48 h.

Proliferation assay—Red blood cells (RBC) were removed from freshly isolated whole spleen cells using ammonium chloride potassium (ACK) lysis buffer for 2 min at room temperature then washed free of lysis buffer using PBS. RBC-depleted spleen cells were then cultured in RPMI 1640 supplemented with 10% FCS (Invitrogen Life Sciences), 1x penicillin/streptomycin/neomycin (Gibco), and 10 mM HEPES buffer (Gibco) at a concentration of 10^6 cells/well in round-bottom 96-well plates at 37 °C. Anti-CD3e (0.05 μg/200 μL well) was added to stimulate cell proliferation in the presence of increasing concentrations of **1** (50 nM, 0.5 μM, 5 μM, and 50 μM). All treatment conditions were controlled to contain a final concentration of 1% DMSO solvent as used in drug preparation. At 72 h of culture, 1 μCu ^{3}H-thymidine (Amersham Biosciences) in 50 μL of media was added per well and allowed to incorporate for 12–16 h. Cells were harvested and washed using an automated cell harvester (Perkin Elmer), and radioactivity was analyzed using a liquid scintillation counter. Cell proliferation is measured as counts per minute (cpm). Permission to use mice for this research project was obtained through the University of Florida IACUC board. Animals were cared for and euthanized according to procedures approved by the IACUC.

NO assay—RAW 264.7 cell assays to measure effects on LPS-induced NO production were performed as previously described.[43]

Antibacterial assays—Activity against *Bacillus cereus*, *Pseudomonas aeruginosa*, and *Mycobacterium tuberculosis* was assessed as we previously described.[44,45]

Supplementary Material

Refer to Web version on PubMed Central for supplementary material.

Acknowledgments

This research was supported by the NIH, NCI grant R01CA172310, and by Shenzhen Peacock Plan (KQTD2015071714043444). We thank many students and staff of the UOGML for assisting VJP with collecting the sample in Guam over the years. We thank Rana Montaser and Yanxia Liu for initial biological testing. We also thank the Harbor Branch Oceanographic Institute at Florida Atlantic University spectroscopy facility for 600 MHz NMR spectrometer time, UV and melting point measurements, and the Florida Atlantic University, Jupiter Campus, for the use of their polarimeter and infrared spectrometer. This is contribution number 1027 from the Smithsonian Marine Station at Fort Pierce. The authors declare the following competing financial interest(s): H. Luesch is co-founder of Oceanyx Pharmaceuticals, Inc., which is negotiating licenses for patents and patent applications related to cyanobacterial metabolites.

References

1. Blunt JW, Copp BR, Keyzers RA, Munro MHG, Prinsep MR. Nat Prod Rep. 2015; 32:116–211. and references therein. [PubMed: 25620233]
2. Liu L, Rein KS. Mar Drugs. 2010; 8:1817–1837. [PubMed: 20631872]
3. Salvador-Reyes LA, Luesch H. Nat Prod Rep. 2015; 32:478–503. [PubMed: 25571978]
4. Erickson KL, Gustafson KR, Pannell LK, Beutler JA, Boyd MR. J Nat Prod. 2002; 65:1303–1306. [PubMed: 12350152]
5. Rao MR, Faulkner DJ. J Nat Prod. 2002; 65:386–388. [PubMed: 11908986]
6. Pereira AR, McCue CF, Gerwick WH. J Nat Prod. 2010; 73:217–220. [PubMed: 20131814]
7. Gutiérrez M, Andrianasolo EH, Shin WK, Goeger DE, Yokochi A, Schemies J, Jung M, France D, Cornell-Kennon S, Lee E, et al. J Org Chem. 2009; 74:5267–5275. [PubMed: 19572575]
8. Gutiérrez M, Tidgewell K, Capson TL, Engene N, Almanza A, Schemies J, Jung M, Gerwick WH. J Nat Prod. 2010; 73:709–711. [PubMed: 20158242]
9. Kwan JC, Meickle T, Ladwa D, Teplitski M, Paul V, Luesch H. Mol Biosyst. 2011; 7:1205–1216. and references therein. [PubMed: 21258753]
10. Barry CS, Bushby N, Charmant JPH, Elsworth JD, Harding JR, Willis CL. Chem Commun. 2005:5097–5099.
11. Chakraborty TK, Reddy VR. Tetrahedron Lett. 2006; 47:2099–2102.
12. Smith AB III, Simov V. Org Lett. 2006; 8:3315–3318. [PubMed: 16836394]
13. Kim H, Hong J. Org Lett. 2010; 12:2880–2883. [PubMed: 20491466]
14. Son JB, Kim SN, Kim NY, Lee DH. Org Lett. 2006; 8:661–664. [PubMed: 16468736]
15. Son JB, Kim SN, Kim NY, Lee DH. Org Lett. 2006; 8:3411.
16. Barry CS, Elsworth JD, Seden PT, Bushby N, Harding JR, Alder RW, Willis CL. Org Lett. 2006; 8:3319–3322. [PubMed: 16836395]
17. Reiff EA, Nair SK, Henri JT, Greiner JF, Reddy BS, Chakrasali R, David SA, Chiu TL, Amin EA, Himes RH, et al. J Org Chem. 2010; 75:86–94. [PubMed: 19954175]
18. Demuth M. Helv Chim Acta. 1978; 61:3136–3138.
19. Mulzer J, Mantoulidis A, Oehler E. J Org Chem. 2000; 65:7456–7467. [PubMed: 11076603]
20. Durgnat JM, Warm A, Vogel P. Synth Commun. 1992; 22:1883–1893.

21. Evans MA, Morken JP. J Am Chem Soc. 2002; 124:9020–9021. [PubMed: 12148984]
22. Storer RI, Takemoto T, Jackson PS, Ley SV. Angew Chem Int Ed. 2003; 42:2521–2525.
23. Gesinski MR, Rychnovsky SD. J Am Chem Soc. 2011; 133:9727–9729. [PubMed: 21639102]
24. Armstrong A, Scutt JN. Org Lett. 2003; 5:2331–2334. [PubMed: 12816441]
25. Armstrong A, Scutt JN. Chem Commun. 2004:510–511.
26. Delhaye L, Merschaert A, Delbeke P, Briône W. Org Process Res Dev. 2007; 11:689–692.
27. Bray CD, Minicone F. Chem Commun. 2010; 46:5867–5869.
28. Kumar P, Dubey A, Harbindu A. Org Biomol Chem. 2012; 10:6987–94. [PubMed: 22832742]
29. Chayajarus K, Chambers DJ, Chughtai MJ, Fairbanks AJ. Org Lett. 2004; 6:3797–3800. [PubMed: 15469352]
30. Collot M, Savreux J, Mallet JM. Tetrahedron. 2008; 64:1523–1535.
31. Millán A, Smith JR, Aggarwal VK. Angew Chemie Int Ed. 2016; 55:2498–2502.
32. Schneider, WP.; McIntosh, AV. US Patent. 2,769,824. 1956.
33. VanRheenen V, Kelly RC, Cha DY. Tetrahedron Lett. 1976; 17:1973–1976.
34. Nicolaou KC, Seitz SP, Papahatjis DP. J Am Chem Soc. 1983; 105:2430–2434.
35. Paquette LA, Barriault L, Pissarnitski D, Johnston JN. J Am Chem Soc. 2000; 122:619–631.
36. Kasai Y, Ito T, Sasaki M. Org Lett. 2012; 14:3186–3189. [PubMed: 22671133]
37. Seden PT, Charmant JPH, Willis CL. Org Lett. 2008; 10:1637–1640. [PubMed: 18355075]
38. Anelli PL, Biffi C, Montanari F, Quici S. J Org Chem. 1987; 52:2559–2562.
39. Inanaga J, Hirata K, Saeki H, Katsuki T, Yamaguchi M. Bull Chem Soc Jpn. 1979; 52:1989–1993.
40. Kusumi S, Tomono S, Okuzawa S, Kaneko E, Ueda T, Sasaki K, Takahashi D, Toshima K. J Am Chem Soc. 2013; 135:15909–15912. [PubMed: 24074200]
41. Schneider U, Schwenk HU, Bornkamm G. Int J Cancer. 1977; 19:621–626. [PubMed: 68013]
42. Fischer BS, Qin D, Kim K, McDonald TV. J Pharmacol Exp Ther. 2001; 299:238–246. [PubMed: 11561085]
43. Ratnayake R, Liu Y, Paul VJ, Luesch H. Cancer Prev Res. 2013; 6:989–999.
44. Montaser R, Abboud KA, Paul VJ, Luesch H. J Nat Prod. 2011; 74:109–112. [PubMed: 21138309]
45. Montaser R, Paul VJ, Luesch H. Phytochemistry. 2011; 72:2068–2074. [PubMed: 21843895]

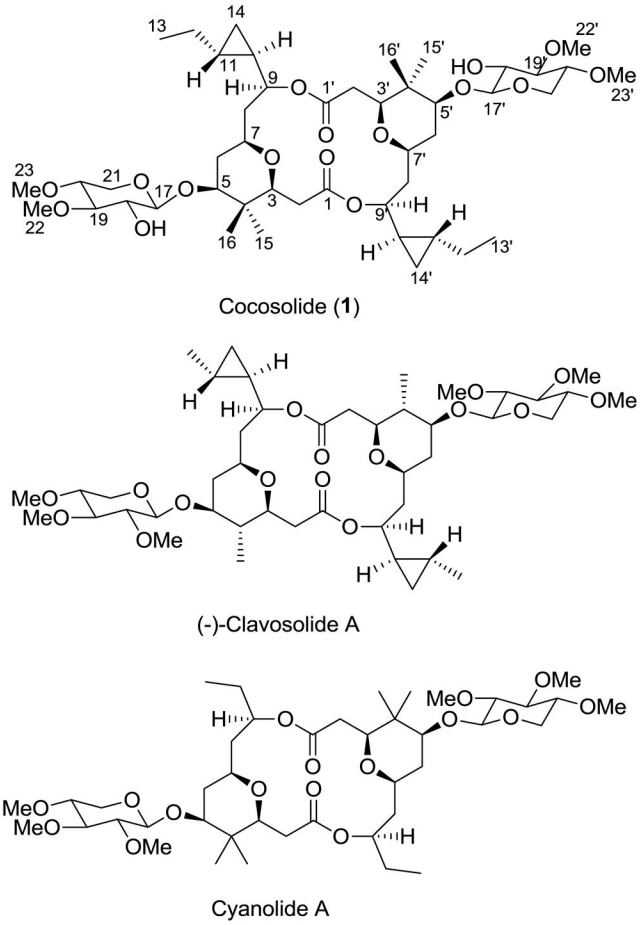

Figure 1.

Structures of cocosolide (**1**) from *Symploca* sp., clavosolide A from the sponge *Myriastra clavosa* and cyanolide A from the cyanobacterium *Lyngbya bouillonii*.

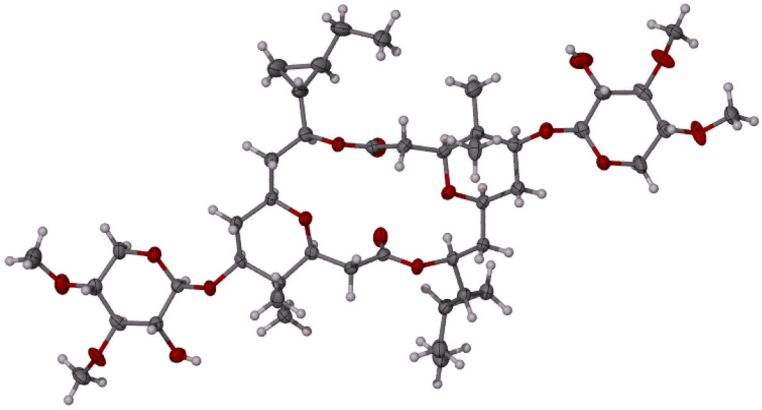

Figure 2.
Computer-generated perspective drawing of the X-ray model of cocosolide (**1**).

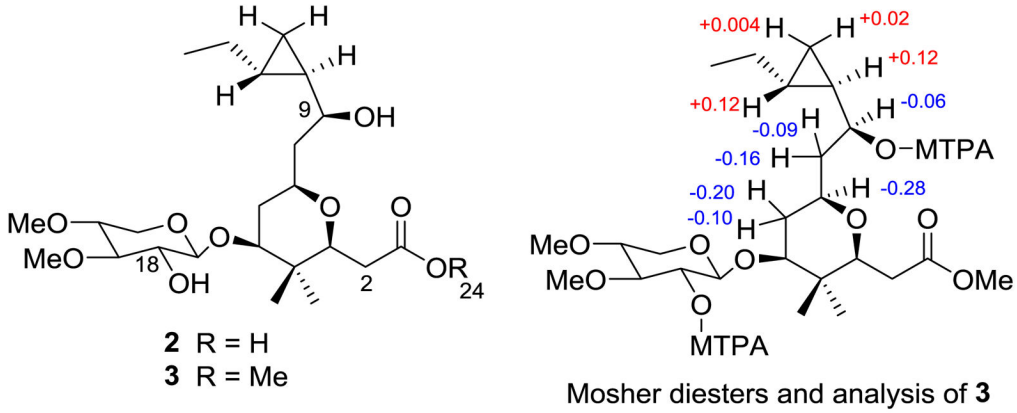

Figure 3.

Base hydrolysis product monomer **2** and corresponding monomer methyl ester **3** used for Mosher's analysis [Δδ (δ_S–δ_R) values shown] and for biological studies.

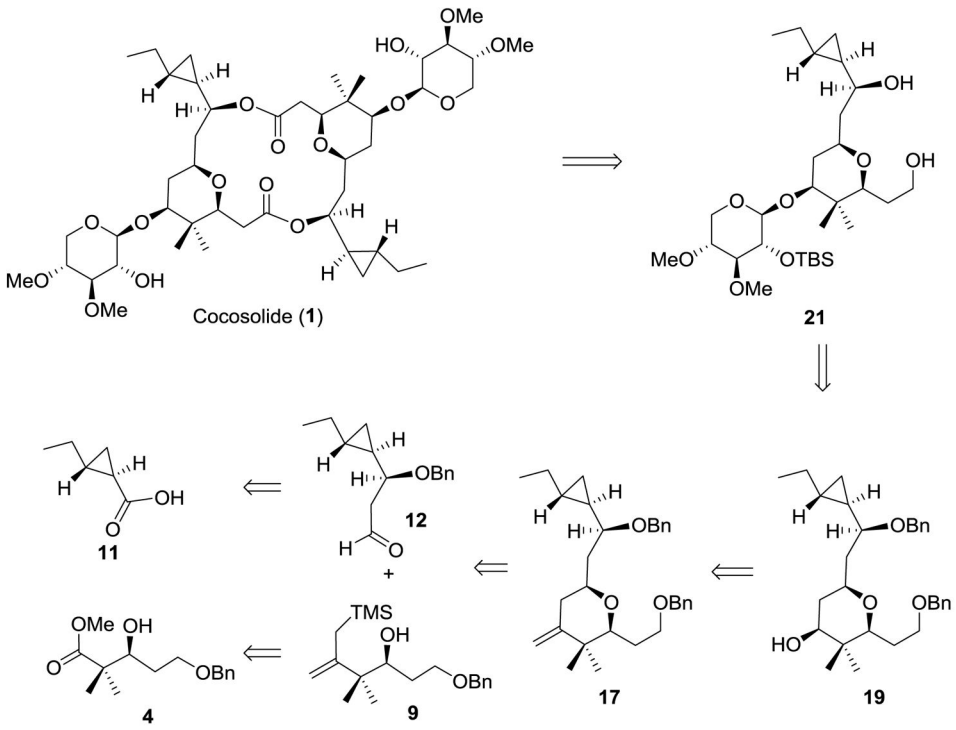

Figure 4.
Retrosynthesis analysis of cocosolide (**1**).

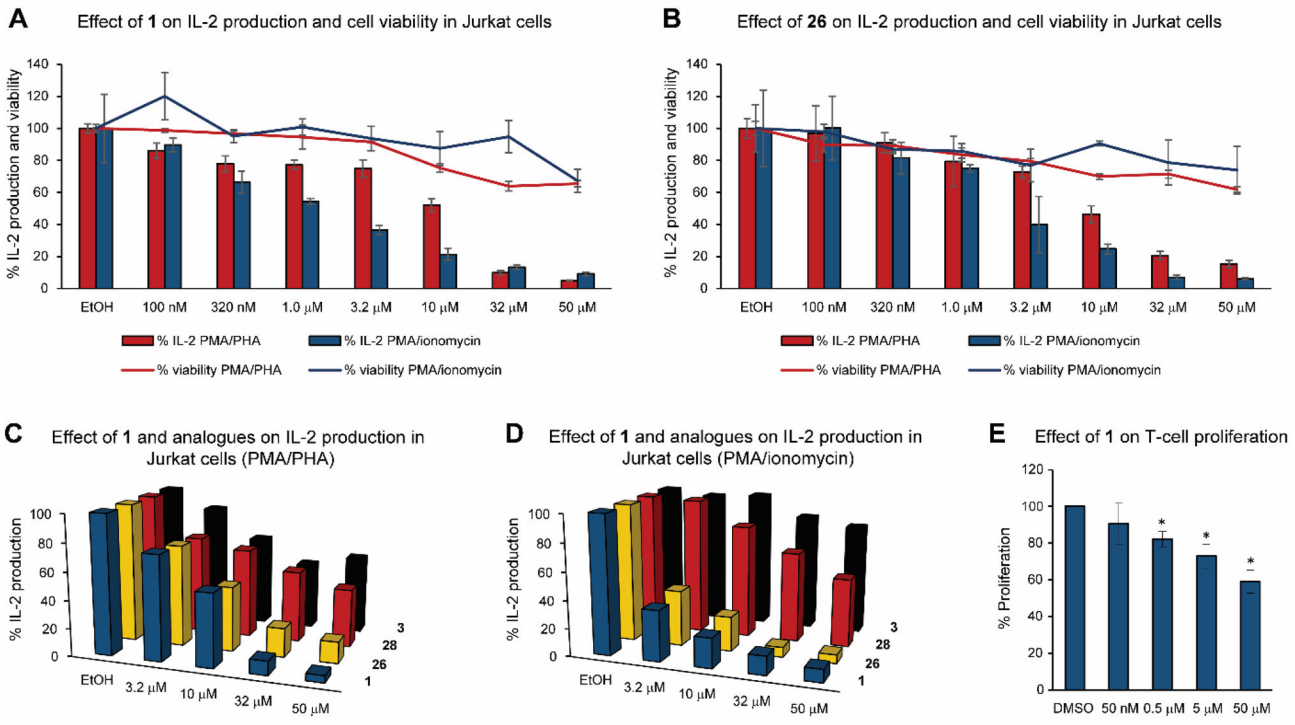

Figure 5.

Biological effects of cocosolide (**1**), [a,a]-anomer **26**, macrocyclic core **28** and monomer methyl ester **3** on T-cell systems. (**A**) Effect of **1** on IL-2 production by Jurkat cells and on cell viability in response to PMA/PHA and PMA/ionomycin stimulation. For comparison, cyclosporine A inhibited both activities at 1 μM by 90%. (**B**) Effect of cocosolide [a,a]-anomer **26** on IL-2 production by Jurkat cells and on cell viability in response to PMA/PHA and PMA/ionomycin stimulation. (**C,D**) Comparison of compounds **1** (natural product), **3** (monomer methyl ester), **26** ([a,a]-anomer) and **28** (aglycon) on their effect on IL-2 production in Jurkat cells (**C**) stimulated by PMA/PHA and (**D**) PMA/ionomycin. (**E**) Spleen cell proliferation assay. Anti-CD3 stimulated cells were cultured in triplicate wells in the presence of increasing concentrations of **1**. Values shown represent the average spleen cell response from the mean triplicate values between two mice. * denotes $p < 0.05$ compared to DMSO.

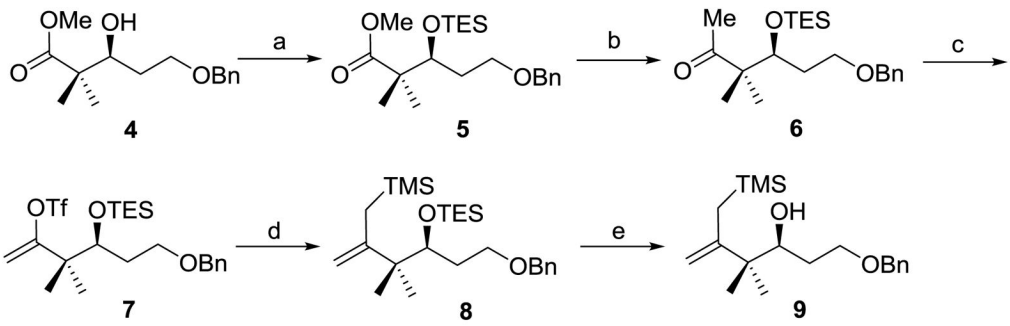

Scheme 1.

Synthesis of allylsilane **9**. a) TESOTf, 2,6-lutidine, DCM, 0 °C, 85%; b) $LiCH_2TMS$, pentane, 0 °C, 98%; c) KHMDS, $PhNTf_2$, THF, −78 °C, 91%; d) $ClMgCH_2TMS$, $Pd(PPh_3)_4$, Et_2O, 0 °C, 81%; e) CSA, MeOH, RT, 75%; DCM=dichloromethane; THF=tetrahydrofuran; TESOTf=triethylsilyl trifluoromethanesulfonate; KHMDS=potassium bis(trimethylsilyl)amide; $PhNTf_2$=*N*-phenyl-bis(trifluoromethanesulfonimide); CSA=10-camphorsulfonic acid.

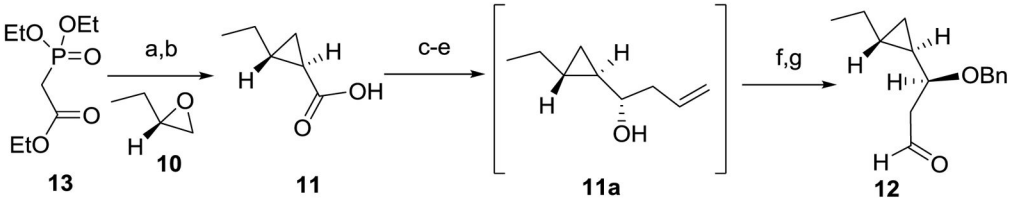

Scheme 2.

Synthesis of aldehyde **12**. a) NaH, toluene, RT, then **10**, 80 °C; b) NaOH (aq.), reflux, 82% (2 steps); c) $LiAlH_4$, THF, 0°C; d) TEMPO, TCCA, DCM, 0 °C; e) (−)IPC_2BOMe, AllylMgBr, Et_2O, (*1R*,*2R*)-2-ethylcyclopropane-1-carbaldehyde, −82 °C to RT, then H_2O_2, NaOH(aq.), reflux; f) BnBr, NaH, THF, 0 °C to RT; g) $NaIO_4$, OsO_4, acetone/H_2O, RT, 26% (5 steps); TEMPO=2,2,6,6-tetramethyl-1-piperidinyloxy; TCCA=trichloroisocyanuric acid; (−)IPC_2BOMe=(−)-*B*-methoxydiisopinocampheylborane.

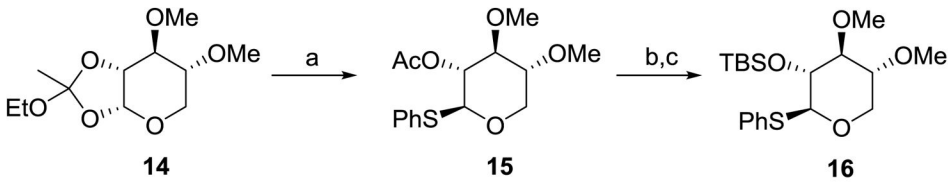

Scheme 3.

Synthesis of thioglycoside **13**. a) PhSH, $BF_3{\cdot}Et_2O$, DCM, RT, 36%; b) NaOMe, MeOH, RT; c) TBSOTf, 2,6-lutidine, DCM, 0 °C, 86% (2 steps); TBSOTf=*tert*-butyldimethylsilyl trifluoromethanesulfonate.

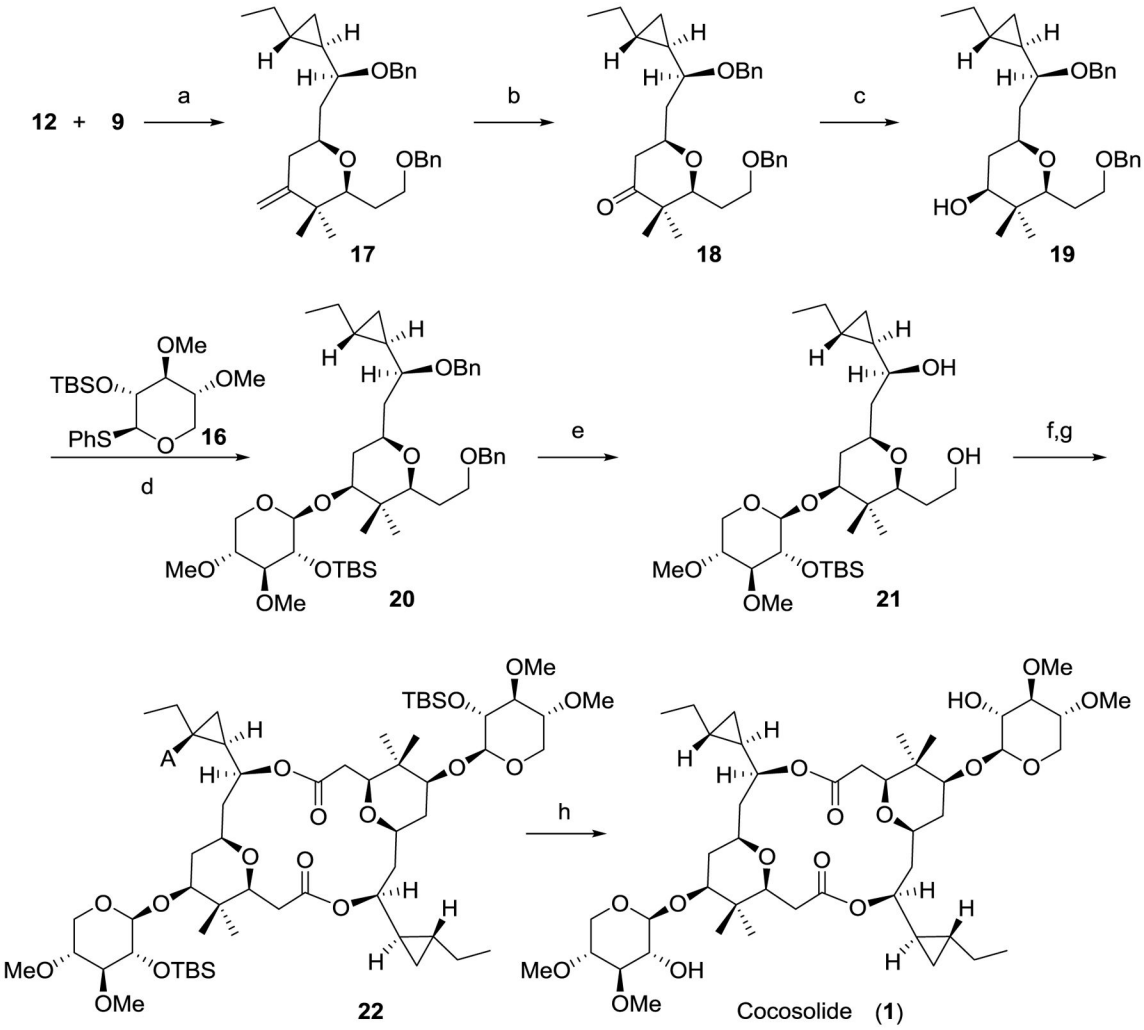

Scheme 4.

Assembly of Subunits and Completion of the Synthesis of Cocosolide (**1**). a) TMSOTf, Et_2O, 4Å MS, −78 °C, 75%; b) OsO_4, NMO, $NaIO_4$, acetone/H_2O, RT, 85%; c) $NaBH_4$, MeOH, −40 °C, 92%; d) NBS, MeCN, then **16**, −25 °C to RT, 60%; e) H_2, Pd/C, MeOH, RT, 83%; f) TEMPO, Bu_4NCl, KBr, NaOCl, $NaHCO_3$, DCM/H_2O, 0 °C; g) 2,4,6-trichlorobenzoyl, DIPEA, RT, then DMAP, toluene, 80 °C, 43% (2 steps); h) TBAF, THF, RT, 82%; TMSOTf=trimethylsilyl trifluoromethanesulfonate; NMO=4-methylmorpholine *N*-oxide; NBS=*N*-bromosuccinimide; DIPEA=*N*,*N*-diisopropylethylamine; DMAP=4-(dimethylamino) pyridine; TBAF= tetra-*n*-butylammonium fluoride.

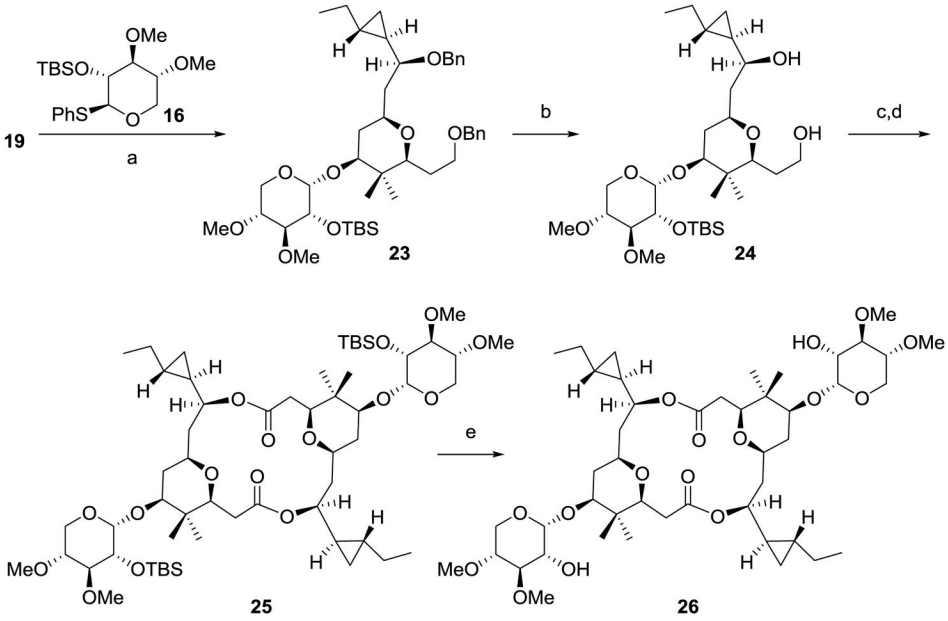

Scheme 5.

Synthesis of [α,α]-anomer of cocosolide (**26**). a) NIS, TfOH, DCM, then **16**, 71%; b) H_2, Pd/C, MeOH, RT, 64%; c) TEMPO, Bu_4NCl, KBr, NaOCl, $NaHCO_3$, DCM/H_2O, 0 °C; d) 2,4,6-trichlorobenzoyl, DIPEA, RT, then DMAP, toluene, 80°C, 40% (2 steps); e) TBAF, THF, RT, 75%; NIS= *N*-iodosuccinimide; TfOH= trifluoromethanesulfonic acid.

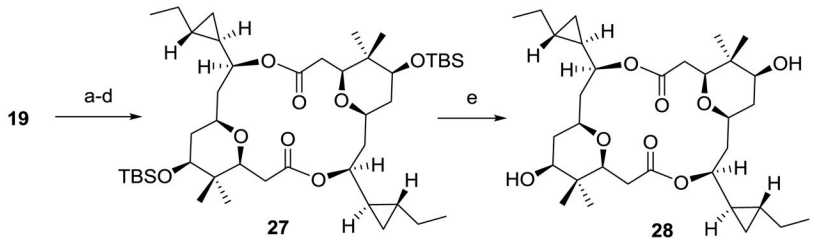

Scheme 6.

Synthesis of macrocyclic core of cocosolide (**28**). a) TBSOTf, 2,6-lutidine, DCM, 0 °C; b) H_2, Pd/C, EtOAc, RT; c) TEMPO, Bu_4NCl, KBr, NaOCl, $NaHCO_3$, DCM/H_2O, 0 °C; d) 2,4,6-trichlorobenzoyl, DIPEA, RT, then DMAP, toluene, 80°C, 19% (4 steps); e) TBAF, THF, RT, 71%.

Table 1

NMR Spectroscopic Data for Cocosolide (1) in CD_3CN (600 MHz)

position	δ_C mult.	δ_H (*J* in Hz)	COSY[a]	HMBC	NOESY[b]
1, 1′	171.7, C			2a, 2b, 3, 9	
2a, 2a′	35.9, CH_2	2.38, dd (17.2, 2.0)	3	3	2b, 3, 15, 16
2b, 2b′		2.07, dd (17.2, 8.2)	3		2a, 3, 15, 16
3, 3′	80.5, CH	3.40, dd (8.2, 2.0)	2a, 2b	2a, 2b, 15, 16	2a, 2b, 15
4, 4′	39.2, C			2a, 5, 6a, 6b 15, 16	
5, 5′	85.1, CH	3.34, dd (11.4, 4.8)	6a, 6b	3, 6, 7, 15, 16	15, 17
6a, 6a′	37.4, CH_2	1.80, m	5, 6b, 7	8a	5, 6b, 7
6b, 6b′		1.35, m	5, 6a, 7		5, 6a
7, 7′	76.3, CH	3.38, m	6a, 6b, 8a, 8b	3, 5, 6a, 6b, 9	8a, 8b, 9
8a, 8a′	41.4, CH_2	1.83, m	7, 8b, 9	6b, 7, 8, 9	8b
8b, 8b′		1.66, ddd (14.3, 4.1, 1.4)	7, 8a, 9		8a
9, 9′	77.6, CH	4.30, dt (8.2, 1.4)	8a, 8b, 10	11, 14a, 14b	7, 10, 14a
10, 10′	24.7, CH	0.68, m	9, 11, 14a, 14b	9, 12a, 12b 14a, 14b	14b
11, 11′	20.6, CH	0.71, m	10, 12a, 12b 14a, 14b	9, 12a, 12b, 13, 14b	9, 12a, 12b
12a, 12a′	27.2, CH_2	1.37, m	11, 12b, 13	10, 13, 14a, 14b	11, 12b, 13
12b, 12b′		0.90, m	11, 12a, 13		11, 12a, 13
13, 13′	13.8, CH_3	0.85, t (6.9)	12a, 12b	11, 12	12a, 12b
14a, 14a′	9.8, CH_2	0.37, dt (8.3, 4.9)	10, 11, 14b	9, 12a, 12b,	9, 11, 14b,
14b, 14b′		0.23, dt (8.3, 4.8)	10, 11, 14a		10, 14a
15, 15′	22.2, CH_3	0.87, s		3, 5, 16	2a, 2b, 3
16, 16′	13.5, CH_3	0.79, s		3, 5, 15	2a, 2b
17, 17′	106.4, CH	4.23, d (7.6)	18	5, 18, 18-OH 19, 21a, 21b	5, 21
18, 18′	74.2, CH	3.18, ddd (8.3, 7.6, 4.8)	17, 19	17, 18-OH, 19	
18, 18′-OH		3.33, d (4.8)			
19, 19′	85.4, CH	3.02, t (8.3)	18, 20	17, 18, 18-OH 20, 21a, 21b, 22	22

Chemistry. Author manuscript; available in PMC 2017 June 06.

position	δ_C mult.	δ_H (*J* in Hz)	COSY[a]	HMBC	NOESY[b]
20, 20′	80.0, CH	3.17, ddd (9.6, 8.3, 4.8)	19, 21a, 21b	18, 19, 21a 21b, 23	21a, 23
21a, 21a′	63.4, CH_2	3.90, dd (11.6, 4.8)	20, 21b	17, 19, 20	20, 21b
21b, 21b′		3.09, dd (11.9, 9.6)	20, 21a		21a
22, 22′	60.4, CH_3	3.49, s		19	19
23, 23′	58.5, CH_3	3.38, s		20	2

[a] ^1H–^1H COSY and proton(s).

[b] NOESY correlations are from proton(s) stated to the indicated protons.